Accepted Manuscript

Genome-wide analysis of *Fusarium verticillioides* reveals inter-kingdom contribution of horizontal gene transfer to the expansion of metabolism

Shan Gao, Scott E. Gold, Jennifer H. Wisecaver, Yong Zhang, Li Guo, Li-Jun Ma, Antonis Rokas, Anthony E. Glenn
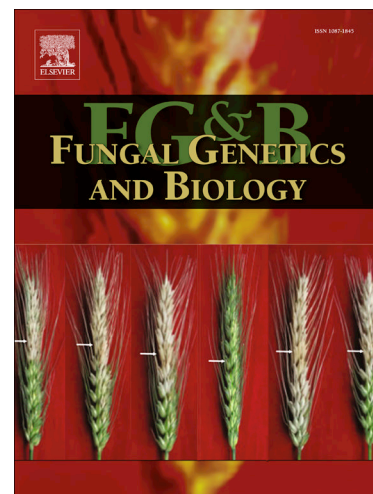
Please cite this article as: Gao, S., Gold, S.E., Wisecaver, J.H., Zhang, Y., Guo, L., Ma, L-J., Rokas, A., Glenn, A.E., Genome-wide analysis of *Fusarium verticillioides* reveals inter-kingdom contribution of horizontal gene transfer to the expansion of metabolism, *Fungal Genetics and Biology* (2019), doi: https://doi.org/10.1016/j.fgb.2019.04.002

Genome-wide analysis of *Fusarium verticillioides* reveals inter-kingdom contribution of horizontal gene transfer to the expansion of metabolism

Shan Gao[a], Scott E. Gold[e,1], Jennifer H. Wisecaver[b,2], Yong Zhang[c], Li Guo[d], Li-Jun Ma[c], Antonis Rokas[b], Anthony E. Glenn[e,1,]*

[a] Department of Plant Pathology, University of Georgia, Athens, GA, USA

[b] Department of Biological Sciences, Vanderbilt University, Nashville, Tennessee, USA

[c] Department of Biochemistry and Molecular Biology, University of Massachusetts, Amherst, Massachusetts, USA

[d] School of Electronics and Information Engineering, Xi'an Jiao Tong University, Xi'an, Shaanxi, China

[e] USDA, ARS, US National Poultry Research Center, Toxicology & Mycotoxin Research Unit, Athens, GA, USA

* Corresponding author.

E-mail address: anthony.glenn@ars.usda.gov (A.E. Glenn).

[1] This research was co-directed by these authors.

[2] Present address: Department of Biochemistry, Purdue Center for Plant Biology, Purdue University, West Lafayette, Indiana, USA

Declarations of interest: none

Abstract

Horizontal gene transfer (HGT) is believed to shape genomes by facilitating the rapid acquisition of adaptive traits. We hypothesized that the economically important fungus *Fusarium verticillioides* is an excellent candidate for investigating the potential impact of HGT on the expansion of metabolic activities given its soilborne nature and versatile lifestyle as both a symptomless endophyte as well as a maize pathogen. To test this hypothesis, we used a phylogenomic pipeline followed by manual curation to perform a genome-wide identification of inter-kingdom derived HGT events. We found strong support for 36 genes in *F. verticillioides* putatively acquired from bacteria. Functional enrichment assessment of these 36 candidates suggested HGT potentially influenced several biochemical activities, including lysine, glycine and nitrogen metabolism. The expression of 25 candidate HGT genes was detected among RNA-Seq datasets from normal and various stress-related growth conditions, thus indicating potential functionality. FVEG_10494, one of the HGT candidates with homologs in only a few *Fusarium* species, was highly and specifically up-regulated under nitric oxide (NO) challenge. Functional analysis of FVEG_10494 suggests the gene moderately enhanced NO-triggered protective responses and suppressed expression of the *F. verticillioides* secondary metabolism gene cluster responsible for production of fusarin C. Overall, our global analysis of HGT events in *F. verticillioides* identified a well-supported set of transferred genes, providing further evidence that HGT offers a mechanism by which fungi can expand their metabolic capabilities, which in turn may enhance their adaptive strategies.

1. Introduction

Horizontal gene transfer (HGT) is the exchange and stable integration of genetic material between different evolutionary lineages (Doolittle, 1999). HGT is rampant in prokaryotes and contributes to observed breaks in species boundaries, generates new biological diversity, and shapes genomes and populations (Doolittle, 1999; Gogarten et al., 2002; Jain et al., 2003; Polz et al., 2013). In eukaryotes HGT is thought to occur at a lower frequency, likely due to the presence of physical barriers such as the nuclear envelope, multicellularity (separate germline and somatic cells), or RNA interference systems (Aramayo and Selker, 2013; Richards et al., 2011). With the rapid increase in publicly accessible eukaryotic genomic data, a growing body of evidence suggests HGT is a factor in the evolution of eukaryotic genomes (Keeling and Palmer, 2008; Richards et al., 2011; Schonknecht et al., 2013; Wijayawardena et al., 2013; Wisecaver and Rokas, 2015; Wisecaver et al., 2014). Several mechanisms have been proposed to explain HGT events in eukaryotes. For example, transposable elements may contribute to HGT by moving or copying genetic material from prokaryotic to eukaryotic genomes (Gilbert and Cordaux, 2013; Walsh et al., 2013). In addition, structural features that facilitate intimate physical contact, such as plant plasmodesmata (Stegemann and Bock, 2009) and fungal anastomoses (Mehrabi et al., 2011), may promote exchange of genetic material between eukaryotes. An interesting recently proposed hypothesis involves lightning-triggered electroporation and electrofusion (Kotnik, 2013) as an additional natural mechanism facilitating HGT.

Fungi are among the eukaryotic groups where many cases of HGT have been described (Kotnik, 2013). The postulated benefits brought to fungi by HGT after functional fixation are the expansion of metabolic networks and osmotrophic capacity (Richards et al., 2011; Slot and Rokas, 2010), promotion of pathogenicity (Ma et al., 2010; de Jonge et al., 2012), enhanced

adaptation to the environment (Cheeseman et al., 2014; Garcia-Vallve et al., 2000; Novo et al., 2009), and gain of secondary metabolic capacity (Glenn et al., 2016; Proctor et al., 2013; Slot and Rokas, 2011; Wisecaver and Rokas, 2015; Wisecaver et al., 2014). The gold standard for HGT inference is phylogenetic analysis with a gene topology that conflicts with the established organismal phylogeny such that the gene of one species or genes from a group of species are nested within sequences derived from distant lineages (Richards et al., 2011). Phylogeny-independent approaches are recommended to further support phylogenetically identified putative HGT events. These include consideration of shared biogeographical/ecological features between species and the detection of genomic regions showing atypical characteristics, such as GC content, compared with the surrounding genome (Fitzpatrick, 2012).

A study examining 60 fully sequenced fungal genomes showed that prokaryotic-derived HGT are especially enriched in Pezizomycotina and scarce in Saccharomycotina (Marcet-Houben and Gabaldon, 2010), leading to the hypothesis that this striking difference might result from distinct lifestyles of these two groups. Consistent with this idea, it has been observed that lifestyles associated with ecological generalists may favor HGT (Marcet-Houben and Gabaldon, 2010), which might be the case for *Fusarium* species. Generally speaking, most *Fusarium* species are soilborne facultative plant pathogens having more diverse lifestyles compared to obligate pathogens. *Fusarium* species cause plant diseases on many field, horticultural, and forest crops in various ecosystems with varying degrees of host specificity (Ma et al., 2013). *Fusarium verticillioides* offers a good model for further evaluation of HGT because it is a soilborne phytopathogen of maize, one of the world's most widely grown and economically important crops, and the fungus can infect maize as a symptomless endophyte that is nearly universally seedborne in kernels (Bacon and Hinton, 1996; Blacutt et al., 2018; Munkvold et al.,

1997). Although previous studies have revealed increasing evidence of HGT events involving

several *Fusarium* species (Campbell et al., 2012; Gardiner et al., 2012; Glenn et al., 2016; Ma et

al., 2010; Proctor et al., 2013; Tsavkelova et al., 2012), including two horizontally transferred

xenobiotic-degrading gene clusters, a thorough analysis of how HGT has shaped the genome of

F. verticillioides has not been conducted.

In this study, we performed a genome-wide analysis of *F. verticillioides* to identify

candidates of HGT using a phylogenomic pipeline. This pipeline was previously reported to

reveal HGT in fructophilic yeasts and in fungal pathogens of animals (Alexander et al., 2016;

Goncalves et al., 2018; Wisecaver et al., 2016). The HGT pipeline generated an initial output of

1,855 candidate genes. Following manual curation, we narrowed this output down to a set of 36

high-confidence HGT candidates that appear to have been acquired from bacteria. Functional

analysis of FVEG_10494, a candidate highly expressed under nitric oxide (NO) challenge and

with homologs in only a few *Fusarium* species, indicated that the gene moderately enhanced

NO-triggered protective responses. Overall the analysis identified a set of high-confidence HGT

candidates and suggested a potential role of HGT events in providing adaptive advantages to *F.*

verticillioides.

2. Materials and methods

2.1 Genome-wide identification of HGT candidates

A phylogenomic pipeline followed by manual screening was conducted to globally reveal

HGT candidates in *F. verticillioides* (Fig. 1). All predicted proteins from the *F. verticillioides*

genome assembly (Ma et al., 2010) were BLASTp queried (e-value = 1, max_target_seqs = 1000)

against a custom database consisting of the National Center for Biotechnology Information

(NCBI) non-redundant protein database (last updated November 24, 2014) plus additional protein sequences from 411 fungal and plant genome assemblies as noted in Alexander et al. (2016). A custom Perl script sorted the BLASTp results based on the normalized bitscore (*nbs*), where *nbs* was calculated as the bitscore of the single best scoring hit sequence divided by the best bitscore possible for the query sequence (i.e. the bitscore of the query aligned to itself). The alien index score (AI) was then calculated for each query protein as modified from Gladyshev et al. (2008). Two taxonomic lineages were first specified: the recipient lineage into which possible HGT events may have occurred (Dikarya, NCBI:txid451864), and a larger clade encompassing the recipient lineage and its sister clades (Opisthokonta, NCBI:txid33154). The AI is given by the formula: AI = *nbsO* – *nbsG*, where *nbsO* is the normalized bitscore of the best hit to a species outside of Opisthokonta, and *nbsG* is the normalized bitscore of the best hit to a species within Opisthokonta (skipping all hits to the recipient Dikarya lineage). The AI is greater than zero if the gene has a better hit to a species outside of Opisthokonta and can be suggestive of either HGT or contamination. Note that the original Gladyshev et al. (2008) AI calculation was based on relative E-values and ranged from −460 to +460, with AI > 45 considered a putative HGT candidate. By converting the AI to a bitscore-based metric, the results are not impacted by BLAST version, database size, or computer hardware. The bitscore-based AI score ranges from +1 to -1, and we considered AI > 0.05 as putative HGT candidates.

HGT candidates identified via the initial AI screen were subjected to downstream phylogenetic analysis. Specifically, for each HGT candidate, we used a Perl script to extract up to 300 homologs from the custom database referenced above based on: a) BLAST similarity (e-value ⩽ 1e-3), b) allowing up to five orders of magnitude difference between query and subject sequence lengths, and c) permitting the inclusion of up to five sequences per species.

Furthermore, to reduce the number of sequences per gene tree, highly similar sequences were collapsed with *CD-HIT* using default parameters (Li and Godzik, 2006). Sequences were aligned with *MAFFT* using the E-INS-i strategy (Katoh and Standley, 2013). The resulting alignment was trimmed with *TRIMAL* using the automated1 strategy (Capella-Gutierrez et al., 2009). Phylogenetic trees were constructed using *FastTree* (Price et al., 2010) with a WAG+CAT amino acid model of substitution, 1000 resamples, four rounds of minimum-evolution subtree-prune-regraft moves (-spr 4), and the more exhaustive maximum likelihood (ML) nearest-neighbor interchange option enabled (-mlacc 2 -slownni).

The phylogenetic trees were then subjected to the first tier of manual curation based on the following criteria. First, the trees must contain at least 20 sequences since misinterpretation of HGT may arise from limited available data and potentially biased sample collection. Second, because the AI score cannot differentiate between HGT donor and recipient, the gene phylogeny must contradict the established species phylogeny, and the transfer direction should be from distantly related taxa to fungi. Third, HGT candidates were further narrowed by BLASTp evaluation to ensure the best hit from the donor group had an e-value $\leqslant$ 1e-30 and bitscore > 40% of the query sequence.

A second tier of manual screening was conducted to ensure strong HGT signals. Specifically, a robust ML topology was inferred for each gene using *RAxML* version 8.0.25 (Stamatakis, 2014) with a PROTGAMMALGF substitution model and rapid bootstrapping (1000 replications). Each gene phylogeny was midpoint rooted and visualized using *iTOL* version 3.0 (Letunic and Bork, 2016). The phylogenies were further screened using the following three filters: 1) the fungal clade inferred to have been the result of HGT must have at least two preceding internal branches with strong bootstrap support (> 80%) nesting the fungi within a

distantly related, non-fungal group of taxa; 2) this group should be predominantly comprised of

taxa belonging to the same class, order, or family; and 3) the overall phylogeny has only a single

fungal clade except where unique exceptions were noted. All genes satisfying these criteria were

subjected to the *in silico* analyses noted below.

2.2 Intron content analysis

The frequency of intron occurrence in the whole genome and in the HGT candidate genes

was determined by the "Exon Count" search strategy in FungiDB (http://fungidb.org) (Stajich et

al., 2012). For example, the rules were set to an exon count of ≥ 1 and ≤ 1 to search for

intronless genes having a single exon. To test if the differences in intron frequency between the

genome and HGT candidates were significant, the Mann‑Whitney-Wilcoxon test was

performed using SAS 9.4 (SAS Institute Inc., Cary, NC, USA).

2.3 Transcriptome profile analysis

The transcriptional profiles of the HGT candidates were examined in 10 *F. verticillioides*

datasets to determine if the genes were expressed and therefore likely functional. This also

allowed us to explore responsive conditions. Included were two RNA sequencing (RNA-Seq)

datasets (Niu et al., 2015; Sikhakolli et al., 2012) extracted from NCBI's Gene Expression

Omnibus (GEO) database (accession numbers GSE61865 and GSE66044) and an additional

eight RNA-Seq datasets from our research groups, including one dataset generated during this

study (see below; GEO Series accession GSE118800), six datasets resulting from exposing *F.

verticillioides* to various xenobiotics (accession GSE116351), and one dataset evaluating

transcriptional response to heat stress (accession GSE113332). The HGT candidates were

considered as expressed genes if they had a FPKM (Fragments Per Kilobase of exon per Million fragments mapped) or RPKM (Reads Per Kilobase of exon per Million fragments mapped) value that was > 2 under normal conditions or a change in expression value of log2 > 1.5 (equivalent to 2.8-fold change; *p*-value < 0.05) under test conditions compared to the untreated control.

2.4 HGT candidate annotation for putative function

The NCBI Conserved Domain Database (https://www.ncbi.nlm.nih.gov/cdd/) was used to determine the possible functions of the proteins encoded by the HGT candidates. The MIPS Functional Catalogue (http://mips.helmholtz-muenchen.de/funcatDB/) was used to identify enriched pathways (*p*-value < 0.05) represented among the HGT candidates compared to the frequency of such pathway genes within the whole *F. verticillioides* genome. The candidates assigned to sub-categories of interest (e.g. nitrogen metabolism, biosynthesis of lysine, etc.) were extracted and further characterized. The subcellular location of encoded proteins was predicted by the TargetP 1.1 Server (http://www.cbs.dtu.dk/services/TargetP/) and further verified by the TMHMM Server v 2.0 (http://www.cbs.dtu.dk/services/TMHMM/). Two web-based tools, *SMURF* (Khaldi et al., 2010) and *antiSMASH* (Medema et al., 2011), were applied to detect the involvement of HGT candidates in secondary metabolism gene clusters. Peroxisomal Targeting Signal 1 prediction was performed using the PTS1 predictor (http://mendel.imp.ac.at/pts1/). Further, the KEGG PATHWAY Database (http://www.genome.jp/kegg/pathway.html) for *F. verticillioides* was referenced to associate possible functions of the proteins. The gene FVEG_09873 was one candidate of interest, and to analyze its potential as a functional diaminopimelate epimerase (EC 5.1.1.7), protein sequences of six of the top BLASTp hits in bacteria (*Escherichia coli* WP_001160654, *Pseudomonas fluorescens* WP_017338124,

Rhizobium sp. WP_007629306, *Burkholderia cepacia* WP_059731579, *Burkholderia pyrrocinia* WP_059973916, and *Burkholderia stagnalis* WP_060148831) were extracted from Uniprot (http://www.uniprot.org/) and aligned using Clustal Omega (http://www.ebi.ac.uk/Tools/msa/clustalo/).

2.5 Fungal and bacterial strains, culture media and growth conditions

Wild-type *F. verticillioides* FRC M-3125 (also known as strain 7600, the sequenced reference strain) was used for genetic and functional characterization. The fungus was grown routinely on potato dextrose agar (PDA; Neogen Food Safety, Lansing, MI, USA) at 27°C in the dark or in potato dextrose broth (PDB; Neogen Food Safety) in a shaker incubator at 250 rpm and 27°C in the dark for three days. For selection of transformed strains, PDA was amended with 150 μg/ml hygromycin B (Invitrogen, Carlsbad, CA, USA) or 300 μg/ml geneticin (Life Technologies, Carlsbad, CA, USA). Minimal medium was made according to Leslie et al. (2006) but without sodium nitrate as nitrogen source (in 1 L: potassium phosphate monobasic, 1 g; magnesium sulfate heptahydrate, 0.5 g; potassium chloride, 0.5 g; trace element solution, 0.2 ml; sucrose, 30 g; agar, 20 g). Various nitrogen sources were added to the minimal medium (see below the section on chemical screening).

For maintenance of the FVEG_10494 gene deletion plasmid (pSG10494_OSCAR), *Escherichia coli* (One Shot® MAX Efficiency® DH5α™-T1R, Invitrogen) was grown in or on Luria Bertani (LB) liquid or agar medium amended with 100 μg/ml spectinomycin (Thermo Fisher Scientific, Waltham, MA, USA) at 37°C overnight. *Agrobacterium tumefaciens* strain AGL-1 was used for fungal transformation and cultured on LB agar amended with 100 μg/ml spectinomycin at 27°C in the dark (Paz et al., 2011).

2.6 Construction of gene deletion mutants and complemented strains

To functionally characterize FVEG_10494, gene deletion mutants as well as complemented strains were created as follows. Deletion plasmid pSG10494_OSCAR was generated for FVEG_10494 using the OSCAR method (Gold et al., 2017; Paz et al., 2011). Supplemental Tables B.1 and B.2 summarize strains and primers used in this study, respectively. Two pairs of primers were designed to amplify about 1 kb of the 5' (primers P7\25 and P7\26) and 3' flanks (primers P7\27 and P7\28) to the gene's open reading frame (ORF). The OSCAR deletion construct contains the two flanks surrounding a hygromycin resistance cassette. The ORF of FVEG_10494 was deleted in strain M-3125 via *Agrobacterium*-mediated transformation (Bundock et al., 1995). Hygromycin-resistant transformants were initially screened by PCR using primers P7\29 and P7\30 for the presence or absence of the FVEG_10494 ORF and using amplification of the Hyg marker gene with primers P1\14 and P1\15 as a positive control. Transformants of interest underwent single-spore purification and were finally screened by PCR for genotype using six pairs of primers (Supplemental Table B.2): i. primer pair P1\14 and P1\15 for presence of the hygromycin resistance cassette, ii. primer pair P7\29 and P7\30 for the loss of the FVEG_10494 ORF, iii. primer pair P7\25 and P1\4 (a primer within the hygromycin resistance cassette) for the presence of the 5' flank, iv. primer pair P7\31 (a primer upstream of the 5' flank sequence of FVEG_10494) and P1\4 for confirmation of homologous recombination of the 5' flank, v. primer pair P1\3 (a primer within the hygromycin resistance cassette) and P7\28 for the presence of the 3' flank, and vi. primer pair P1\3 and P7\32 (a primer downstream of the 3' flank sequence of FVEG_10494) for confirmation of homologous recombination of the

3' flank. Deletion strains Δ10494-6.1 and Δ10494-6.4 (Supplemental Table B.1) were confirmed

by Southern hybridization as noted below.

Complemented strains were constructed via lithium acetate-mediated cotransformation

(Bourett et al., 2002). The wild-type FVEG_10494 amplicon (total length 5059 bp) was

generated with primers P7\33 and P7\34 (Supplemental Table B.2) to include the ORF (2841 bp)

and both upstream (911 bp) of the predicted start codon and downstream (1307 bp) of the stop

codon. Both the wild-type amplicon and the *Not*I digested selection vector pGEN-NotI (1 μg)

were cotransformed into lithium acetate treated competent cells (Bourett et al., 2002) of the

deletion strain Δ10494-6.4. Transformants were selected on 300 μg/ml geneticin and 150 μg/ml

hygromycin B and further confirmed by PCR with primer pairs P7\29 and P7\30 and P1\37 and

P1\38 (Supplemental Table B.2) for the presence of the FVEG_10494 ORF and the geneticin

cassette.

2.7 Southern hybridization

To confirm the loss of the target gene, Southern hybridization was conducted as follows.

Total genomic DNA was extracted from 4-day-old PDB liquid cultures of *F. verticillioides* wild

type and transformants using the DNeasy Plant Mini Kit (Qiagen Inc., Valencia, CA) following

the manufacturer's protocol. The extracted DNA was digested with *Kpn*I (New England Biolabs,

Ipswich, MA, USA). A total of 1.5 μg digested genomic DNA was separated on a 0.8% agarose

0.5X Tris-Borate-EDTA gel and blotted onto a Hybond-N+ nylon membrane (Amersham

Biosciences, Buckinghamshire, England). Probes hybridizing to the coding sequence of

FVEG_10494 (using primers P7\29 and P7\30) and the hygromycin cassette (using primers

P1\14 and P1\15) were amplified using the PCR DIG Probe Synthesis Kit (Roche Diagnostics,

Indianapolis, IN, USA). The first round of hybridization was performed using the FVEG_10494

probe following the DIG application manual (Roche Diagnostics). The probe-target hybrids were

detected by chemiluminescent assay and visualized with an Alpha Innotech FluorChem 8000

digital imaging system with a 40-min exposure (Supplemental Fig. A.2.a). The ORF probe was

stripped with alkaline buffer and the membrane was reprobed with the hygromycin cassette

probe. The probe-target hybrids were detected as described above (Supplemental Fig. A.2.b).

2.8 Chemical screening

Since the protein sequence of FVEG_10494 contains domains homologous to the type II

homoserine kinase involved in threonine metabolism and the 4-aminobutyrate aminotransferase

involved in γ-aminobutyric acid (GABA) metabolism, a chemical screening assay containing

compounds associated with either threonine or GABA metabolism was conducted. Strains M-

3125, Δ10494-6.4 and Δ10494-6.4::C3.1 were grown in PDB for three days. The spores were

harvested and washed twice with sterile deionized water, followed by dilution to 10^6 spores/ml.

Agar-based nitrogen-limited minimal medium was supplemented with selected compounds,

autoclaved and then aliquoted to 6-well culture plates (Corning, NY, USA). The tested

compounds (Sigma-Aldrich Chemical Co., Milwaukee, WI, USA) included L-glutamic acid (0.5

mg/ml), GABA (0.5 mg/ml), L-alanine (0.5 mg/ml), glycine (0.5 mg/ml), L-aspartic acid (0.45

mg/ml), L-threonine (0.5 mg/ml), and L-methionine (0.5 mg/ml). Ten μl of 10^6 spores/ml

suspension were inoculated at the center of each well, and the plates were sealed and incubated

at 27°C for three days. Each strain was assessed in triplicate on each substrate.

2.9 RNA extraction and qRT-PCR analysis

Transcriptional analysis was used to test the response of FVEG_10494 to nitric oxide (NO). The fungus was inoculated into 3 ml PDB buffered with 0.1 M sodium phosphate and cultured at 250 rpm and 27°C for three days in Falcon 14 mL polypropylene round-bottom tubes (Corning Science México, Reynosa, TM, México). One ml of culture was transferred to lysing matrix S tubes (MP Biomedicals, LLC, Santa Ana, CA, USA), centrifuged at 10,000 x g for 5 min at 4°C, and the supernatant discarded. Lysis buffer (PureLink® RNA Mini Kit, Thermo Fisher Scientific) was immediately added to the fungal pellets, and the samples were homogenized using the FastPrep-24™ 5G Instrument (MP Biomedicals) at a speed of 6 m/sec with two segments of homogenization for 30 seconds with a 1 min rest in between. Total RNA was extracted following the manufacturer's instructions (PureLink® RNA Mini Kit, Thermo Fisher Scientific). NO treated samples were cultured the same way in PDB buffered with 0.1 M sodium phosphate for three days followed by 30 min exposure to 1.5 mM diethylenetriamine (DETA) NONOate (Cayman chemical, Ann Arbor, MI, USA) dissolved in 0.01 M NaOH, and the samples were then harvested for RNA extraction as stated above. Three biological replicates were included for each treatment.

For quantitative reverse transcription-PCR (qRT-PCR), isolated RNA samples were DNase treated (TURBO DNA-free™ Kit, Thermo Fisher Scientific), tested by conventional PCR for the complete removal of DNA, and checked for quality (RNA integrity number > 6.0) using an Agilent 2100 Bioanalyzer (Agilent Technology, Waldbronn, Germany). Complementary DNA synthesis and qRT-PCR were carried out using a one-step qRT-PCR Kit (SuperScript® III Platinum® SYBR® Green One-Step qRT-PCR Kit, Thermo Fisher Scientific) in triplicate. The data were normalized to the expression level of β-tubulin (FVEG_04081) and calculated via the

$2^{-\Delta\Delta Ct}$ method (Livak and Schmittgen, 2001). The primers used for this assay are shown in Supplemental Table B.2.

2.10 RNA sequencing and analysis

Total fungal RNA was isolated and checked for quality as stated above. Twelve libraries (wild type and single mutant Δ10494-6.4 treated with and without 1.5 mM DETA NONOate for 30 min, with three biological replicates each) were prepared and sequenced on an Illumina NextSeq (75 Cycles) High Output Flow Cell (paired end, 75 bp read length) by the Georgia Genomics Facility. Raw RNA-Seq reads were subject to quality control by *FastQC* (http://www.bioinformatics.babraham.ac.uk/projects/fastqc/), followed by removal of low quality reads (Phred score < 20) and Illumina sequencing adapters using *Trimmomatic* 0.25 (Bolger et al., 2014). Mapping of the filtered paired-end reads against the *F. verticillioides* 7600 genome (Ma et al., 2010) (Fusarium verticillioides_7600_3_supercontig; www.fungidb.org) was performed using the *align* function in the *Rsubread* package (Liao et al., 2013) in Bioconductor (www.bioconductor.org). Read counting, normalization, and expression level (FPKM) calculations were executed using the *featurecount* function in *Rsubread* using the default settings. Differential gene expression analysis was then performed using *edgeR* (Robinson et al., 2010) and *DESeq* (Anders and Huber, 2010) packages, by applying a false discovery rate threshold of <0.05 for the adjusted *p*-value. The log2 threshold was set to 1 (equivalent to 2-fold) to screen for differentially expressed genes. Annotations were predicted using the NCBI Conserved Domain Database and Pedant-Pro (http://pedant.helmholtz-muenchen.de/pedant3htmlview/ pedant3view?Method=analysis&Db=p3_p15553_Fus_verti_v31).

3. Results

3.1 Identification of HGT candidates and genomic features

The BLAST-based AI screen identified an initial set of 1,855 potential HGT candidate genes in *F. verticillioides* (Fig. 1). Subsequent two-tiered manual inspection reduced the HGT candidates to 36 genes (Table 1). Sixteen of the gene trees passed all three of the second-tier criteria and were considered as strong HGT candidates. The additional 20 gene phylogenies met two of the three criteria from the second tier of curation and were considered as probable HGT candidates. All 36 genes were subjected to *in silico* analyses as outlined below, and the information for each gene is summarized in Table 1 and Supplemental Table B.3. *RAxML* maximum likelihood phylogenies for these 36 genes are shown in Appendix C. The phylogenies suggested that all 36 genes were acquired from bacteria.

Given the high frequency of bacterial origin of these HGT candidates, we hypothesized they should have fewer introns than the overall *F. verticillioides* genome. In fact, 30 of the 36 candidates (83%) lacked introns, compared to 26% of genes in the whole genome that are intronless (Mann–Whitney-Wilcoxon test, Z = -1.8913, *p* = 0.0293; Supplemental Tables B.4 and B.5). There are 16,240 genes annotated within the genome of *F. verticillioides* as detailed in the FungiDB and NCBI databases. The density of genes per chromosome, calculated by dividing the total number of genes on each chromosome by the size (Mbp) of the chromosome, ranged from approximately 366 to 461 (Supplemental Fig. A.3.a). Chromosome 1, the largest chromosome at 6.22 Mbp, had the smallest gene density at 366, and chromosomes 10 and 11, which are the smallest chromosomes at 2.26 and 2.04 Mbp, respectively, had the highest gene densities at 461 and 443, respectively. We also calculated the density of intronless genes on the chromosomes (Supplemental Fig. A.3.b). A total of 4279 genes lack introns as noted in

Supplemental Table B.5, and the greatest densities of these intronless genes were found on chromosomes 8 (136 genes/Mbp), 10 (157 genes/Mbp), and 11 (134 genes/Mbp). Further, gene density analysis showed an enrichment of the 36 HGT candidates on chromosomes 4, 10, and 11 with 1.7, 1.8, and 2.0 HGTs/Mbp, respectively, compared to a range of 0.2 to 1.3 HGTs/Mbp on the other chromosomes (Supplemental Fig. A.3.c).

To further assess genomic features of the HGT candidates, two web-based tools, *SMURF* and *anti-SMASH*, were used to predict whether any of the genes are associated with known or predicted secondary metabolism biosynthetic gene clusters. Both *SMURF* and *anti-SMASH* predictions suggested two candidates, FVEG_03408 and FVEG_10494, are localized within putative secondary metabolism gene clusters (Supplemental Table B.6). In addition, *anti-SMASH* also predicted that gene FVEG_09873 is associated with a biosynthetic gene cluster.

3.2 Transcriptome profiling analysis

A series of *F. verticillioides* RNA-Seq datasets from various physiological and xenobiotic-challenged conditions was screened to determine whether the HGT candidates were expressed (Supplemental Table B.7). Of the 36 HGT candidates, 25 were expressed under at least one of the experimental conditions examined, suggesting their potential functionality, though perhaps under specific conditions. For example, 15 of the HGT candidates were differentially expressed when exposed to physiological or xenobiotic stresses, and among these were FVEG_10494 and FVEG_12273, which were expressed only under stress conditions. FVEG_10494 had a log2 fold change of 12.2 in response to nitric oxide exposure, and FVEG_12273 had a log2 fold change of 5.7 in response to chlorzoxazone, one of several xenobiotic compounds we've tested against *F. verticillioides* as part of a separate study.

3.3 HGT candidates are enriched in lysine, glycine and nitrogen metabolic pathways

To gain insight into the general functions encoded by the horizontally transferred genes, we used the MIPS Functional Catalogue (FunCat) website (Ruepp et al., 2004) and identified 21 of the 36 HGT candidates associated with the following enriched functional categories: metabolism (01), glycolysis and gluconeogenesis (02.01), complex cofactor/cosubstrate/vitamin binding (16.21), electron transport (20.01.15), activity of intercellular mediators (40.02.03), and the peroxisome (42.19) (Supplemental Table B.8). Table 2 summarizes the distribution of these HGT candidates among the functional categories and the degree of their enrichment compared to the genome wide frequency of each category within *F. verticillioides*. All 21 of the functionally annotated candidates were predicted to be involved in metabolism, with 10 of the genes also distributed in additional functional categories. Table 3 illustrates the distribution of gene candidates in the enriched sub-categories of metabolism and the degree of enrichment compared to the genome as a whole. The sub-categories of sphingolipid metabolism and utilization of vitamins and cofactors were the most enriched despite each containing only one HGT candidate. Although carbohydrate metabolism and secondary metabolism contained 10 and 5 candidates, respectively, the degree of fold enrichment compared to the whole genome was only 2.2 and 2.6. Thus, the enriched subcategories of amino acid metabolism (lysine and glycine) and nitrogen metabolism were selected for further characterization since they each contained several genes with approximately 6-fold enrichment over the genome as a whole.

Regarding lysine metabolism, two distinct pathways are responsible for lysine biosynthesis in nature, the diaminopimelate (DAP) pathway and the α-aminoadipate (AAA) pathway, with the DAP pathway commonly found in bacteria and plants and the AAA pathway

almost exclusively limited to fungi (Torruella et al., 2009; Zabriskie and Jackson, 2000). To

better understand genes that may contribute to lysine biosynthesis in *F. verticillioides*, we

mapped them to the KEGG PATHWAY Database (Fig. 2). Presence of vertically inherited genes

required in each step of the AAA pathway suggested that *F. verticillioides* successfully exploits

this pathway for lysine biosynthesis. In contrast, the DAP pathway is incomplete, only having

genes encoding the first steps in this pathway (Fig. 2; presence of vertically inherited genes is

indicated with green boxes), yet two HGT candidates were associated with the DAP pathway

based on functional annotations (Table 1). FVEG_00154 putatively encodes a

dihydrodipicolinate synthase (EC 4.3.3.7), but its expression was not detected in the

transcriptional data (Supplemental Table B.7). The fungus does have a vertically inherited

dihydrodipicolinate synthase encoded by FVEG_05936, and therefore any expression of

FVEG_00154 may be particular to unknown specific conditions. The second HGT candidate

gene, FVEG_09873, is an orphan gene only found in *F. verticillioides* and no other fungus, and it

putatively encodes a DAP epimerase (EC 5.1.1.7) catalyzing the stereoinversion of L,L-DAP to

D,L-*meso*-DAP, a precursor to both L-lysine in the DAP pathway and peptidoglycan in bacteria

(Hor et al., 2013). FVEG_09873 is localized on the assembled *F. verticillioides* chromosome 1

contig CM000578.1 (Supplemental Fig. A.4), and its neighboring genes are homologous to genes

in other *Fusarium* species. Therefore, it is unlikely that FVEG_09873 is a sequencing artifact of

bacterial contamination. The maximum likelihood phylogeny of FVEG_09873 suggested it was

acquired by *F. verticillioides* from plant-associated Proteobacteria (Appendix C; see also Table

1). Although currently available transcriptional data did not support expression of FVEG_09873

(Supplemental Table B.7), analysis of a multiple sequence alignment with protein sequences

from six bacteria showed that most of the key sites (e.g. binding site and active site) are intact

(Supplemental Fig. A.5), suggesting the predicted protein encoded by FVEG_09873 might still function as a DAP epimerase, although specific expression may be dependent on currently unknown conditions.

A total of four HGT candidates (FVEG_03408, FVEG_08761, FVEG_10494, and FVEG_13277) were associated with metabolism of glycine based on FunCat prediction (Table 1; Supplemental Table B.8). Both FVEG_03408 and FVEG_13277 (57% identity in protein sequence) were potentially acquired from actinobacteria and are predicted to encode sarcosine oxidases, which catalyze the oxidative demethylation of sarcosine to directly yield glycine. FunCat prediction also indicated these two genes as possibly associated with lysine metabolism. Further, the two genes were also assigned to the peroxisome (42.19) category, and the Peroxisomal Targeting Signal 1 (PTS1) prediction suggested the sarcosine oxidase encoded by FVEG_13277 might be a peroxisomal matrix protein. As noted above, both *SMURF* and *anti-SMASH* predictions suggest the involvement of FVEG_03408 in an NRPS-like secondary metabolism gene cluster (Supplemental Table B.6). For gene FVEG_08761 that putatively encodes a glycine/D-amino acid oxidase involved in the degradation of glycine to glyoxylate (Table 1), it was identified as an anciently transferred candidate from proteobacteria and has homologs in several *Fusarium*, *Aspergillus* and *Penicillium* species. The fourth gene, FVEG_10494, was the focus of functional studies and will be discussed later in detail.

Interestingly, FunCat prediction also suggested FVEG_08761, FVEG_10494, and FVEG_13277 may be involved with metabolism of nitrogen, along with FVEG_11816 and FVEG_12262 (Table 1; Supplemental Table B.8). These last two genes were not associated with any other metabolism sub-category. FVEG_11816 putatively encodes an aspartate ammonia lyase (aspartase) with high protein sequence similarity ($\leqslant 66\%$) to proteobacteria and had

limited distribution to species of *Fusarium*, *Aspergillus*, and *Penicillium*. FVEG_12262 likely

encodes a subgroup of the nitrilase superfamily and may be involved in nutrient assimilation or

detoxification of nitrile compounds. It also has high protein sequence identity to bacteria ($\leqslant$

70%) and is more broadly distributed among fungi.

3.4 The 16 genes having the strongest support for HGT into F. verticillioides

As noted above, of the 36 genes identified by the phylogenomic pipeline and manual

curation, only 16 of the gene phylogenies met all of the assigned criteria and therefore were

considered to be the strongest HGT candidates (Table 1). Four genes (FVEG_04320,

FVEG_07753, FVEG_10494 and FVEG_03450) have homologs only in other *Fusarium* species,

and all showed strong support for their derivation from bacteria based on phylogenetic analysis

(Appendix C) and high protein sequence identity (67-77%; Table 1). For instance, FVEG_03450

nested within many genes derived from plant-associated *Rhizobium* and *Sinorhizobium* species.

The HGT candidate FVEG_10494, along with its homologs in the other cereal-infecting

Fusarium pathogens, contains three conserved protein domains, namely a type II homoserine

kinase, a domain of unknown function (DUF3549), and a GABA aminotransferase. Phylogenetic

analysis showed FVEG_10494 falls within a clade exclusive to cereal-infecting *Fusarium*

species nested within a larger clade of *Microbacterium* and other actinomycetes (Fig. 3;

Appendix C). In addition, the GC content of FVEG_10494 (Fig. 4.a) is distinctly elevated

(59.2%) compared to its neighboring genes in the *F. verticillioides* genome (49.3% averaged

over the six genes upstream and four genes downstream). Moreover, FVEG_10494 is 76%

identical at the amino acid level to the homolog from *Microbacterium testaceum*, which is an

endophyte of corn and sorghum (Zinniel et al., 2002). Reciprocal BLASTp of the *M. testaceum*

homolog indicated the homologous proteins in *Fusarium* were the most similar. The common

niche within corn and possible intimate contact between *Microbacterium* and *Fusarium* may

have facilitated a horizontal transfer event. Due to these details, in combination with its potential

involvement in a predicted secondary metabolism gene cluster (Supplemental Table B.6) and its

dramatic induction under NO exposure (Fig. 4.b), we focused on functional characterization of

FVEG_10494 by deleting the gene. More details are presented below.

The remaining 12 of the 16 strongest HGT candidates have homologs in broader fungal

lineages (Table 1), suggesting that the postulated transfer events were more ancient. For example,

both FVEG_08362 and FVEG_11008 encode putative monoamine oxidases that share 58%

amino acid identity to each other. Phylogenetic analysis suggested these two genes cluster with

the same set of *Fusarium* sequences and nest within similar bacterial sequences (Appendix C). It

is likely there was one lateral transfer event from actinobacteria to a common fungal ancestor

followed by gene duplication, giving rise to FVEG_08362 and FVEG_11008 and other fungal

homologs.

3.5 Functional characterization of FVEG_10494

Given the limited information on FVEG_10494 and its homologs, we approached its

characterization in two ways: 1) screening mutants on chemical compounds based on the

predicted annotation and pathways that may be potentially involved; and 2) identifying genes

interacting with or influenced by FVEG_10494 via transcriptional analyses.

3.5.1 Chemical screening suggested FVEG_10494 might not be related to annotated functions

As already noted, the FVEG_10494 predicted protein contains the three conserved

domains of a type II homoserine kinase, a domain of unknown function (DUF3549), and a

GABA aminotransferase. Homoserine kinase catalyzes the ATP-dependent phosphorylation of L-homoserine to L-homoserine phosphate and is important in the biosynthesis of threonine (Kingsbury and McCusker, 2010), while GABA aminotransferase (also known as GABA transaminase) deaminates GABA to form succinate semialdehyde. To test if FVEG_10494 is functionally associated with the above pathways, wild-type strain M-3125, gene deletion strain Δ10494-6.4, and complemented strain Δ10494-6.4::C3.1 were grown on nitrogen-limited minimal media individually amended with selected compounds involved in GABA and threonine metabolism as the sole nitrogen source. We did not observe overt differences among the strains grown on any of these compounds (Supplemental Fig. A.6), suggesting that FVEG_10494 may not play a large role in the threonine and GABA pathways or that it is redundant with other genes under the conditions tested. Predictions indicate *F. verticillioides* has a single vertically inherited homoserine kinase (FVEG_03006) and two GABA aminotransferases (FVEG_05239 and FVEG_06940) based on searches of FungiDB followed by BLASTp confirmation. Interestingly, only FVEG_05239 exhibited differential expression in both wild type (log2 fold change = 1.8) and the Δ10494 mutant (log2 fold change = 2.8) when the strains were exposed to NO compared to their respective non-treated controls. The two-fold greater induction in the mutant compared to wild type may be indicative of compensatory activity. Lastly, it is worth noting that the complemented strain Δ10494-6.4::C3.1 did have a very subtle difference in colony morphology on L-threonine, showing slightly enhanced growth with more aerial hyphae compared to M-3125 and the deletion strain Δ10494-6.4 (Supplemental Fig. A.6). The complemented strain may possess multiple functional inserts of the FVEG_10494 gene, thus providing enhanced metabolic activity. This will be investigated further as a separate study.

3.5.2 FVEG_10494 is highly induced under nitric oxide (NO) exposure

A previous unpublished transcriptional study conducted by our group indicated

FVEG_10494 was one the most up-regulated genes when *F. verticillioides* was challenged with

1.5 mM DETA NONOate, a NO donor (NCBI Gene Expression Omnibus accession GSE56827).

To validate the observed 157-fold induction in that microarray study, qRT-PCR was performed

on 3-day-old PDB cultured cells of wild type treated with or without 30 min exposure to 1.5 mM

DETA NONOate. Relative expression analysis suggests that FVEG_10494 in PDB liquid culture

was barely transcribed (averaged Ct = 30) but was dramatically increased over 900-fold in NO-

exposed samples (Fig. 4.b). This level of FVEG_10494 expression in response to NO indicated a

potential role in nitrosative stress, yet when the Δ10494-6.4 mutant was exposed to various

concentrations of the NO-donor DETA NONOate, we did not observe any adverse effects on

growth compared to wild type (data not shown).

3.5.3 FVEG_10494 impacts expression of the fusarin C biosynthetic gene cluster and also NO-
responsive detoxification genes

To assess how FVEG_10494 affects *F. verticillioides* under nitrosative stress, we

conducted RNA-Seq analysis on wild-type strain M-3125 compared to the gene deletion mutant

Δ10494-6.4 treated with and without 1.5 mM DETA NONOate. A summary of RNA-Seq results

is shown in Table 4, and the corresponding lists of differentially expressed genes are provided in

Appendix D. FVEG_10494 was the most up-regulated gene when wild type was challenged with

the NO-donor molecule DETA NONOate (log2 fold change = 12.2, or 4622-fold). Moreover,

there were no differentially expressed genes except for FVEG_10494 itself between PDB-grown

untreated deletion mutant Δ10494-6.4 and wild-type strain M-3125. The transcriptional

comparison between the two strains when challenged with NO identified 13 up-regulated and 16

down-regulated genes (including FVEG_10494) in the deletion mutant (Table 5 and Appendix

D). The log2 fold change values were mostly < 2 (11 of the 13 up-regulated genes) or > -2 (15 of the 16 down-regulated genes) in the NO-exposed deletion mutant when compared to NO-exposed wild type (Table 5). The moderate transcriptional changes suggested that FVEG_10494, even when expressed at a high level, only moderately impacts the expression of a small number of genes in *F. verticillioides*.

Among the 13 up-regulated genes in the challenged deletion mutant, six genes encode proteins containing no known conserved domains (Table 5; FVEG_08732, FVEG_09672, FVEG_09673, FVEG_10117, FVEG_10576, and FVEG_16635). Five of the up-regulated genes (FVEG_11078, FVEG_11079, FVEG_11080, FVEG_11085 and FVEG_11086) belong to the secondary metabolite biosynthetic gene cluster for the mycotoxin fusarin C (Brown et al., 2012). This indicates that FVEG_10494 may play a role in the suppression of the fusarin C biosynthetic gene cluster during NO exposure. We did not observe any such differential expression effects on other secondary metabolite gene clusters.

Most of the genes down-regulated in the NO-challenged deletion mutant encode proteins involved in either cellular transport or nitrosative/oxidative stress based on predicted annotations using MIPS FunCat (Table 5; Supplemental Table B.9). Functional enrichment analysis also suggested that genes related to cellular transportation and detoxification appear more frequently (range of approximately 3- to 179-fold enrichment) among the down-regulated genes than those in the overall genome (Supplemental Table B.9). Figure 5 shows that for 11 of the down-regulated genes in Table 5, the absence of FVEG_10494 dampened their induction upon NO challenge in the mutant compared to wild type. Four of the down-regulated genes in Table 5 (FVEG_09142, FVEG_12249, FVEG_13989, and FVEG_15302) are not shown in Figure 5 because their differential expression in one or more of the comparisons was not significant based

on adjusted *p*-value (< 0.5). Overall the data suggest that FVEG_10494 may moderately enhance the efficiency of NO-triggered responses in *F. verticillioides* and thus help the fungus to better overcome such environmental stress.

4. Discussion

As a soilborne fungus demonstrating versatile roles in the ecosystem, ranging from a symptomless systemic endophyte to a necrotrophic pathogen, *F. verticillioides* likely has ample opportunity to develop intimate contact with its host and other microbes (Blacutt et al., 2018; Gao et al., 2017). This diversity of interactions may elevate its susceptibility as a recipient of alien genetic materials. In this study, we implemented an automatic phylogenomic pipeline followed by two rounds of manual curation to reveal 36 HGT candidates of high confidence. These candidates include not only recent transfers (e.g. from bacteria to *Fusarium*) but also more ancient transfers (e.g. from bacteria to Ascomycota). The performance of a series of *in silico* analyses revealed shared or enriched structural and metabolic features of the HGT candidates compared to general genome attributes. For instance, 30 of the 36 HGT candidates lacked any introns, a finding consistent with the intronless structure of most bacterial genes, thus supporting their postulated bacterial origin.

In this study, we were particularly interested in inter-kingdom HGT candidates in *F. verticillioides* that were acquired from distant taxa, such as bacteria. As a future follow up to this study, we could focus on genes in *F. verticillioides* acquired from other fungal lineages, with a particular focus on genes that may be associated with virulence, adaption, and secondary metabolite gene clusters. In fact, numerous reports have shown fungal-to-fungal HGT events conferring potential advantageous traits (Ma et al., 2010; Wisecaver and Rokas, 2015). For

example, an entire cluster consisting of 23 genes for the production of sterigmatocystin was horizontally transferred from *Aspergillus nidulans* to *Podospora anserina* (Slot and Rokas, 2011). Another compelling example is the horizontal transfer of the toxin-encoding gene *ToxA* from the wheat pathogen *Stagonospora nodorum* in the 1940s to another pathogenic fungus, *Pyrenophora tritici-repentis* (Friesen et al., 2006). In addition, a recent study by our group suggests that two xenobiotic-degrading gene clusters in *F. verticillioides* were horizontally transferred to other fungi independently (Glenn et al., 2016). Similar genomic environments and regulatory machinery may facilitate such intra-kingdom fungal HGT events of whole gene clusters. In contrast, genes acquired across kingdoms by fungi are largely single genes (Gardiner et al., 2013). The clustering of genes encoding linked metabolic functions has been indicated to be both an evolutionary consequence and driving force of HGT in fungal genomes (Walton, 2000).

The acquisition and eventual fixation of a foreign gene in a recipient's genome is a multi-step process including: 1) transfer of genes with genomic features typical of the donor lineage, 2) maintenance and replication of the transferred genes, 3) spread of the genes within the population of the recipient, and 4) amelioration to the genome of the recipient lineage (Eisen, 2000). It is reasonable to assume that the evolutionary distance between donor and recipient can impact the degree of transferred sequence modification. In the case of prokaryote-to-eukaryote transfer, adjustments of genomic features, including gene promoters, intron-splicing systems, or GC content and codon usage, need to be modified to optimize function in the recipient genome (amelioration). This may lead to lower sequence identity of the eukaryote query to the prokaryotic homologs than that involving prokaryote-to-prokaryote HGT. In our study, the amino acid sequence identities ranged from 44% to 77% for the 16 best-supported HGT candidates compared to their highest scoring bacterial homologs in BLASTp results.

It is predicted that in order for an acquired gene to be retained it should function in the new lineage and preferably contribute advantages to the recipient. Our analysis indicated that 25 of the 36 HGT candidates we identified were expressed under at least one tested condition. What's more, two HGT candidates, FVEG_10494 and FVEG_12273, were distinctly induced upon exposure to stressed conditions (FVEG_10494 in response to NO, and FVEG_12273 in response to chlorzoxazone). This observation led to the hypothesis that some horizontally acquired genes may only be beneficial under specific environmental conditions, enhancing survival through imposed bottlenecks and contributing quantitatively to the overall fitness of *F. verticillioides*. FVEG_10494, for example, had the highest induction when wild type was treated with NO, yet the gene only moderately enhanced the efficiency of NO-triggered responses in *F. verticillioides* as suggested by the narrow range of genes with affected expression in the RNA-Seq analysis of the Δ10494-6.4 mutant. Additionally, the mutant did not exhibit any changes in sensitivity to NO. Further, although FVEG_10494 has well-supported conserved protein domains, the chemical screen assays conducted with the Δ10494-6.4 mutant did not indicate any essential functions related to type II homoserine kinase or GABA aminotransferase activity. The elevated induction of FVEG_05239, encoding a putative GABA aminotransferase, in the Δ10494 mutant compared to the induction in wild type when both strains were treated with NO may be indicative of redundant functions with possible compensatory response from FVEG_05239 in the absence of FVEG_10494. Conversely, creating a deletion strain for FVEG_05239 and quantifying the expression of FVEG_10494 might provide some indication of whether FVEG_10494 can compensate for FVEG_05239. In addition to such gene deletion experiments, creation of an over-expression strain for FVEG_10494 could indicate if the encoded protein

provides an additive metabolic benefit. Such a possibility will be investigated as part of future studies.

The FVEG_10494 homolog in *F. pseudograminearum* (FPSE_07765) was previously noted as a potential horizontally acquired gene with 75% identity at the amino acid level to a protein from *M. testaceum* (Gardiner et al., 2012), which is an actinobacterial endophyte of maize, sorghum, and various other plants (Zinniel et al., 2002). We also noted the close phylogenetic relationship of FVEG_10494 and its homologs to the protein from *M. testaceum* and other *Microbacterium* species. The elevated GC content of intronless FVEG_10494 (59.2%) compared to its neighboring genes in the *F. verticillioides* genome is further evidence of its potential bacterial origin.

RNA-Seq revealed a small number of differentially expressed genes in the Δ10494 deletion mutant when challenged with NO. Five of the genes (FVEG_11078, FVEG_11079, FVEG_11080, FVEG_11085 and FVEG_11086) are part of the fusarin C biosynthetic gene cluster, and they were up-regulated slightly in the NO-treated Δ10494 mutant. Interestingly, these genes were slightly down-regulated in wild type when exposed to NO (data not shown). The differential expression of only some of the genes within the cluster is interesting. A previous study of the *Fusarium fujikuroi* genes within its fusarin C cluster suggested that homologs of FVEG_11078, FVEG_11079, FVEG_11085 and FVEG_11086 were sufficient for the production of fusarin C (Niehaus et al., 2013). The remaining cluster genes were not essential. The biological basis for the differential expression of the fusarin C gene cluster during NO exposure is unclear since no physiological or ecological function has been attributed to this secondary metabolite.

As for the down-regulated genes in the NO-challenged deletion mutant, predicted annotations of the encoded proteins suggest they function in cellular transportation and nitrosative/oxidative stress. For instance, FVEG_04238 encodes a protein similar to Flr1, a plasma membrane transporter involved in the efflux of multiple drugs in *Saccharomyces cerevisiae* (Alarco et al., 1997; Broco et al., 1999; Jungwirth et al., 2000). As another example, the predicted protein of FVEG_03830 is related to the bifunctional Ure2 in *S. cerevisiae* that is associated not only with nitrogen catabolite repression when ample nitrogen sources are available (Coschigano and Magasanik, 1991), but also oxidative stress (Rai and Cooper, 2005; Rai et al., 2003), which is likely to occur during exposure to NO.

Consistent with a previous study (Richards et al., 2011), functional category analysis revealed an enriched number of HGT candidates in amino acid, nitrogen, and other forms of metabolism, suggesting these transfers may benefit *F. verticillioides* by expanding such processes in the fungus. One example may be the putative DAP epimerase encoding gene FVEG_09873. Multiple sequence alignment of the protein from *F. verticillioides* and the sequences from six bacteria, including a reference *E. coli* sequence, showed that most of the key sites (e.g. binding and active sites) are retained in the *F. verticillioides* protein. The *E. coli* reference sequence did differ from *F. verticillioides* and the other bacterial sequences at one binding site (position 11 in the *E. coli* sequence) and one active site (position 217). A pair of active site cysteine residues (Cys73 and Cys217) were proposed to be responsible for the epimerase stereoinversion reaction that respectively deprotonates L,L-DAP and reprotonates the resulting intermediate to produce D,L-*meso*-DAP (Koo et al., 2000). Although C217 is instead a serine in the encoded proteins of FVEG_09873 and five representative bacteria, the putative DAP epimerase may still be functional given that a C217S mutant protein in *E. coli* can still

function, though with a noticeable drop in enzyme activity, because cysteine residues in proximity to C217 may compensate as the second active site (Koo et al., 2000). Previously, a study on the evolution of lysine biosynthesis suggested that *lysA*, a core gene in the DAP pathway encoding diaminopimelate decarboxylase, may have been acquired by some eukaryotes from eubacteria (Torruella et al., 2009). As with the case of *F. verticillioides*, these eukaryotes also do not contain a complete set of genes required for the DAP pathway. Such DAP pathway genes in organisms lacking the capability to fully utilize the pathway are worth further study with regard to conditions favoring gene expression and heterologous expression in model bacteria to confirm functionality.

One potential explanation for the existence of incomplete metabolic pathways in fungi is the utilization of certain biochemical components by symbiotic bacteria. Recent studies have shown the impact of such bacteria on the biology, virulence, and production of secondary metabolites by their fungal hosts. For instance, studies of the ectosymbiotic bacteria associated with nonpathogenic isolates of *F. oxysporum* showed that the bacteria reduce expression of fungal genes responsible for successful penetration of host plant roots (Minerdi et al., 2008) and modulate the production of small volatile organic compounds that protect plants from pathogenic *F. oxysporum* (Minerdi et al., 2009; Minerdi et al., 2011). Additional examples are the "mycotoxin" producing endofungal bacteria *Burkholderia rhizoxinica* and *B. endofungorum* that are both associated with the zygomycete *Rhizopus microspores* and responsible for the production of rhizoxin, the causative agent of rice seedling blight, and rhizonin, a hepatotoxic cyclopeptide, respectively (Lackner et al., 2009). Therefore, it is reasonable to speculate that symbiotic bacteria may be capable of utilizing certain fungal metabolic pathways for their own

benefit. More importantly, physically intimate bacterial-fungal associations could facilitate HGT of metabolic genes from bacteria to fungi.

To summarize our findings in this study, we revealed the occurrence of HGT candidates in *F. verticillioides* via a flexible and semi-automatic phylogenomic pipeline, and further assessed the functional and genomic attributes of these candidate genes. Subsequent studies focusing on additional detailed characterization of interesting HGT candidates may support their potential contribution to *F. verticillioides* by conferring adaptive metabolic advantages.

Acknowledgements

Appendix A. Supplementary figures

Additional experimental data were provided in the supplemental material section (Figures A.1–A.6). Supplementary data associated with this article can be found, in the online version, at http://.

Appendix B. Supplementary tables

Additional details on the *F. verticillioides* HGT candidates are provided in the

supplemental material section (Tables B.1–B.9). Supplementary data associated with this article

can be found, in the online version, at http://.

Appendix C. Supplementary phylogenies

RAxML phylogenies for the 36 most robust representatives of HGT in *F. verticillioides*.

Supplementary data associated with this article can be found, in the online version, at http://.

Appendix D. Supplementary lists of differentially expressed genes

RNA-Seq analysis was conducted on wild-type strain M-3125 compared to the gene

deletion mutant Δ10494-6.4 treated with and without 1.5 mM DETA NONOate, and the

corresponding lists of differentially expressed genes are provided. Supplementary data associated

with this article can be found, in the online version, at http://.

References

Alarco, A. M., Balan, I., Talibi, D., Mainville, N., Raymond, M., 1997. AP1-mediated multidrug resistance in *Saccharomyces cerevisiae* requires *FLR1* encoding a transporter of the major facilitator superfamily. J. Biol. Chem. 272, 19304-19313.

Alexander, W. G., Wisecaver, J. H., Rokas, A., Hittinger, C. T., 2016. Horizontally acquired genes in early-diverging pathogenic fungi enable the use of host nucleosides and nucleotides. Proc. Natl. Acad. Sci. U.S.A. 113, 4116-4121.

Anders, S., Huber, W., 2010. Differential expression analysis for sequence count data. Genome Biol. 11, R106.

Aramayo, R., Selker, E. U., 2013. *Neurospora crassa*, a model system for epigenetics research. Cold Spring Harb. Perspect. Biol. 5, a017921.

Bacon, C. W., Hinton, D. M., 1996. Symptomless endophytic colonization of maize by *Fusarium moniliforme*. Can. J. Bot. 74, 1195-1202.

Blacutt, A. A., Gold, S. E., Voss, K. A., Gao, M., Glenn, A. E., 2018. *Fusarium verticillioides*: Advancements in understanding the toxicity, virulence, and niche adaptations of a model mycotoxigenic pathogen of maize. Phytopathology 108, 312-326.

Bolger, A. M., Lohse, M., Usadel, B., 2014. Trimmomatic: a flexible trimmer for Illumina sequence data. Bioinformatics 30, 2114-2120.

Bourett, T. M., Sweigard, J. A., Czymmek, K. J., Carroll, A., Howard, R. J., 2002. Reef coral fluorescent proteins for visualizing fungal pathogens. Fungal Genet. Biol. 37, 211-220.

Broco, N., Tenreiro, S., Viegas, C. A., Sa-Correia, I., 1999. *FLR1* gene (ORF YBR008c) is required for benomyl and methotrexate resistance in *Saccharomyces cerevisiae* and its

benomyl-induced expression is dependent on pdr3 transcriptional regulator. Yeast 15**,** 1595-1608.

Brown, D. W., Butchko, R. A. E., Busman, M., Proctor, R. H., 2012. Identification of gene clusters associated with fusaric acid, fusarin, and perithecial pigment production in *Fusarium verticillioides*. Fungal Genet. Biol. 49**,** 521-532.

Bundock, P., den Dulk-Ras, A., Beijersbergen, A., Hooykaas, P. J., 1995. Trans-kingdom T-DNA transfer from *Agrobacterium tumefaciens* to *Saccharomyces cerevisiae*. EMBO J. 14**,** 3206-3214.

Campbell, M. A., Rokas, A., Slot, J. C., 2012. Horizontal transfer and death of a fungal secondary metabolic gene cluster. Genome Biol. Evol. 4**,** 289-293.

Capella-Gutierrez, S., Silla-Martinez, J. M., Gabaldon, T., 2009. trimAl: a tool for automated alignment trimming in large-scale phylogenetic analyses. Bioinformatics 25**,** 1972-1973.

Cheeseman, K., Ropars, J., Renault, P., Dupont, J., Gouzy, J., Branca, A., Abraham, A. L., Ceppi, M., Conseiller, E., Debuchy, R., Malagnac, F., Goarin, A., Silar, P., Lacoste, S., Sallet, E., Bensimon, A., Giraud, T., Brygoo, Y., 2014. Multiple recent horizontal transfers of a large genomic region in cheese making fungi. Nat. Commun. 5**,** 2876.

Coschigano, P. W., Magasanik, B., 1991. The *URE2* gene product of *Saccharomyces cerevisiae* plays an important role in the cellular response to the nitrogen source and has homology to glutathione s-transferases. Mol. Cell. Biol. 11**,** 822-832.

de Jonge, R., van Esse, H. P., Maruthachalam, K., Bolton, M. D., Santhanam, P., Saber, M. K., Zhang, Z., Usami, T., Lievens, B., Subbarao, K. V., Thomma, B. P., 2012. Tomato immune receptor Ve1 recognizes effector of multiple fungal pathogens uncovered by genome and RNA sequencing. Proc. Natl. Acad. Sci. U.S.A. 109**,** 5110-5115.

Doolittle, W. F., 1999. Lateral genomics. Trends Cell Biol. 9, M5-8.

Eisen, J. A., 2000. Horizontal gene transfer among microbial genomes: new insights from complete genome analysis. Curr. Opin. Genet. Dev. 10, 606-611.

Fitzpatrick, D. A., 2012. Horizontal gene transfer in fungi. FEMS Microbiol. Lett. 329, 1-8.

Friesen, T. L., Stukenbrock, E. H., Liu, Z., Meinhardt, S., Ling, H., Faris, J. D., Rasmussen, J. B., Solomon, P. S., McDonald, B. A., Oliver, R. P., 2006. Emergence of a new disease as a result of interspecific virulence gene transfer. Nat. Genet. 38, 953-956.

Gao, M., Glenn, A. E., Blacutt, A. A., Gold, S. E., 2017. Fungal lactamases: Their occurrence and function. Front. Microbiol. 8, 1775.

Garcia-Vallve, S., Romeu, A., Palau, J., 2000. Horizontal gene transfer of glycosyl hydrolases of the rumen fungi. Mol. Biol. Evol. 17, 352-361.

Gardiner, D. M., Kazan, K., Manners, J. M., 2013. Cross-kingdom gene transfer facilitates the evolution of virulence in fungal pathogens. Plant Sci. 210, 151-158.

Gardiner, D. M., McDonald, M. C., Covarelli, L., Solomon, P. S., Rusu, A. G., Marshall, M., Kazan, K., Chakraborty, S., McDonald, B. A., Manners, J. M., 2012. Comparative pathogenomics reveals horizontally acquired novel virulence genes in fungi infecting cereal hosts. PLoS Pathog. 8, e1002952.

Gilbert, C., Cordaux, R., 2013. Horizontal transfer and evolution of prokaryote transposable elements in eukaryotes. Genome Biol. Evol. 5, 822-832.

Gladyshev, E. A., Meselson, M., Arkhipova, I. R., 2008. Massive horizontal gene transfer in bdelloid rotifers. Science 320, 1210-1213.

Glenn, A. E., Davis, C. B., Gao, M., Gold, S. E., Mitchell, T. R., Proctor, R. H., Stewart, J. E., Snook, M. E., 2016. Two horizontally transferred xenobiotic resistance gene clusters

associated with detoxification of benzoxazolinones by *Fusarium* species. PLoS One 11**,** e0147486.

Gogarten, J. P., Doolittle, W. F., Lawrence, J. G., 2002. Prokaryotic evolution in light of gene transfer. Mol. Biol. Evol. 19**,** 2226-2238.

Gold, S. E., Paz, Z., Garcia-Pedrajas, M. D., Glenn, A. E., 2017. Rapid deletion production in fungi via *Agrobacterium* mediated transformation of OSCAR deletion constructs. J. Vis. Exp. 124**,** e55239.

Goncalves, C., Wisecaver, J. H., Kominek, J., Oom, M. S., Leandro, M. J., Shen, X. X., Opulente, D. A., Zhou, X., Peris, D., Kurtzman, C. P., Hittinger, C. T., Rokas, A., Goncalves, P., 2018. Evidence for loss and reacquisition of alcoholic fermentation in a fructophilic yeast lineage. Elife 7**,** e33034.

Hor, L., Dobson, R. C., Downton, M. T., Wagner, J., Hutton, C. A., Perugini, M. A., 2013. Dimerization of bacterial diaminopimelate epimerase is essential for catalysis. J. Biol. Chem. 288**,** 9238-9248.

Jain, R., Rivera, M. C., Moore, J. E., Lake, J. A., 2003. Horizontal gene transfer accelerates genome innovation and evolution. Mol. Biol. Evol. 20**,** 1598-1602.

Jungwirth, H., Wendler, F., Platzer, B., Bergler, H., Hogenauer, G., 2000. Diazaborine resistance in yeast involves the efflux pumps Ycf1p and Flr1p and is enhanced by a gain-of-function allele of gene *YAP1*. Eur. J. Biochem. 267**,** 4809-4816.

Katoh, K., Standley, D. M., 2013. MAFFT multiple sequence alignment software version 7: improvements in performance and usability. Mol. Biol. Evol. 30**,** 772-780.

Keeling, P. J., Palmer, J. D., 2008. Horizontal gene transfer in eukaryotic evolution. Nat. Rev. Genet. 9**,** 605-618.

Khaldi, N., Seifuddin, F. T., Turner, G., Haft, D., Nierman, W. C., Wolfe, K. H., Fedorova, N. D., 2010. SMURF: Genomic mapping of fungal secondary metabolite clusters. Fungal Genet. Biol. 47**,** 736-741.

Kingsbury, J. M., McCusker, J. H., 2010. Homoserine toxicity in *Saccharomyces cerevisiae* and *Candida albicans* homoserine kinase (thr1Delta) mutants. Eukaryot. Cell 9**,** 717-728.

Koo, C. W., Sutherland, A., Vederas, J. C., Blanchard, J. S., 2000. Identification of active site cysteine residues that function as general bases: Diaminopimelate epimerase. J. Am. Chem. Soc. 122**,** 6122-6123.

Kotnik, T., 2013. Lightning-triggered electroporation and electrofusion as possible contributors to natural horizontal gene transfer. Phys. Life Rev. 10**,** 351-370.

Lackner, G., Partida-Martinez, L. P., Hertweck, C., 2009. Endofungal bacteria as producers of mycotoxins. Trends Microbiol. 17**,** 570-576.

Leslie, J. F., Summerell, B. A., Bullock, S., 2006. The *Fusarium* Laboratory Manual. Wiley.

Letunic, I., Bork, P., 2016. Interactive tree of life (iTOL) v3: an online tool for the display and annotation of phylogenetic and other trees. Nucleic Acids Res. 44**,** W242-245.

Li, W., Godzik, A., 2006. Cd-hit: a fast program for clustering and comparing large sets of protein or nucleotide sequences. Bioinformatics 22**,** 1658-1659.

Liao, Y., Smyth, G. K., Shi, W., 2013. The Subread aligner: fast, accurate and scalable read mapping by seed-and-vote. Nucleic Acids Res. 41**,** e108.

Livak, K. J., Schmittgen, T. D., 2001. Analysis of relative gene expression data using real-time quantitative PCR and the 2-$\Delta\Delta$CT method. Methods 25**,** 402-408.

Ma, L. J., Geiser, D. M., Proctor, R. H., Rooney, A. P., O'Donnell, K., Trail, F., Gardiner, D. M., Manners, J. M., Kazan, K., 2013. *Fusarium* pathogenomics. Annu. Rev. Microbiol. 67**,** 399-416.

Ma, L. J., van der Does, H. C., Borkovich, K. A., Coleman, J. J., Daboussi, M. J., Di Pietro, A., Dufresne, M., Freitag, M., Grabherr, M., Henrissat, B., Houterman, P. M., Kang, S., Shim, W. B., Woloshuk, C., Xie, X., Xu, J. R., Antoniw, J., Baker, S. E., Bluhm, B. H., Breakspear, A., Brown, D. W., Butchko, R. A., Chapman, S., Coulson, R., Coutinho, P. M., Danchin, E. G., Diener, A., Gale, L. R., Gardiner, D. M., Goff, S., Hammond-Kosack, K. E., Hilburn, K., Hua-Van, A., Jonkers, W., Kazan, K., Kodira, C. D., Koehrsen, M., Kumar, L., Lee, Y. H., Li, L., Manners, J. M., Miranda-Saavedra, D., Mukherjee, M., Park, G., Park, J., Park, S. Y., Proctor, R. H., Regev, A., Ruiz-Roldan, M. C., Sain, D., Sakthikumar, S., Sykes, S., Schwartz, D. C., Turgeon, B. G., Wapinski, I., Yoder, O., Young, S., Zeng, Q., Zhou, S., Galagan, J., Cuomo, C. A., Kistler, H. C., Rep, M., 2010. Comparative genomics reveals mobile pathogenicity chromosomes in *Fusarium*. Nature 464**,** 367-373.

Marcet-Houben, M., Gabaldon, T., 2010. Acquisition of prokaryotic genes by fungal genomes. Trends Genet. 26**,** 5-8.

Medema, M. H., Blin, K., Cimermancic, P., de Jager, V., Zakrzewski, P., Fischbach, M. A., Weber, T., Takano, E., Breitling, R., 2011. antiSMASH: rapid identification, annotation and analysis of secondary metabolite biosynthesis gene clusters in bacterial and fungal genome sequences. Nucleic Acids Res. 39**,** W339-346.

Mehrabi, R., Bahkali, A. H., Abd-Elsalam, K. A., Moslem, M., Ben M'barek, S., Gohari, A. M., Jashni, M. K., Stergiopoulos, I., Kema, G. H., de Wit, P. J., 2011. Horizontal gene and

chromosome transfer in plant pathogenic fungi affecting host range. FEMS Microbiol. Rev. 35, 542-554.

Minerdi, D., Bossi, S., Gullino, M. L., Garibaldi, A., 2009. Volatile organic compounds: a potential direct long-distance mechanism for antagonistic action of *Fusarium oxysporum* strain MSA 35. Environ. Microbiol. 11, 844-854.

Minerdi, D., Bossi, S., Maffei, M. E., Gullino, M. L., Garibaldi, A., 2011. *Fusarium oxysporum* and its bacterial consortium promote lettuce growth and expansin A5 gene expression through microbial volatile organic compound (MVOC) emission. FEMS Microbiol. Ecol. 76, 342-351.

Minerdi, D., Moretti, M., Gilardi, G., Barberio, C., Gullino, M. L., Garibaldi, A., 2008. Bacterial ectosymbionts and virulence silencing in a *Fusarium oxysporum* strain. Environ. Microbiol. 10, 1725-1741.

Munkvold, G. P., McGee, D. C., Carlton, W. M., 1997. Importance of different pathways for maize kernel infection by *Fusarium moniliforme*. Phytopathology 87, 209-217.

Niehaus, E. M., Kleigrewe, K., Wiemann, P., Studt, L., Sieber, C. M., Connolly, L. R., Freitag, M., Guldener, U., Tudzynski, B., Humpf, H. U., 2013. Genetic manipulation of the *Fusarium fujikuroi* fusarin gene cluster yields insight into the complex regulation and fusarin biosynthetic pathway. Chem. Biol. 20, 1055-1066.

Niu, C., Payne, G. A., Woloshuk, C. P., 2015. Transcriptome changes in *Fusarium verticillioides* caused by mutation in the transporter-like gene *FST1*. BMC Microbiol. 15, 90.

Novo, M., Bigey, F., Beyne, E., Galeote, V., Gavory, F., Mallet, S., Cambon, B., Legras, J. L., Wincker, P., Casaregola, S., Dequin, S., 2009. Eukaryote-to-eukaryote gene transfer

events revealed by the genome sequence of the wine yeast *Saccharomyces cerevisiae* EC1118. Proc. Natl. Acad. Sci. U.S.A. 106**,** 16333-16338.

Paz, Z., García-Pedrajas, M. D., Andrews, D. L., Klosterman, S. J., Baeza-Montañez, L., Gold, S. E., 2011. One Step Construction of Agrobacterium-Recombination-ready-plasmids (OSCAR), an efficient and robust tool for ATMT based gene deletion construction in fungi. Fungal Genet. Biol. 48**,** 677-684.

Polz, M. F., Alm, E. J., Hanage, W. P., 2013. Horizontal gene transfer and the evolution of bacterial and archaeal population structure. Trends Genet. 29**,** 170-175.

Price, M. N., Dehal, P. S., Arkin, A. P., 2010. FastTree 2--approximately maximum-likelihood trees for large alignments. PLoS One 5**,** e9490.

Proctor, R. H., Van Hove, F., Susca, A., Stea, G., Busman, M., van der Lee, T., Waalwijk, C., Moretti, A., Ward, T. J., 2013. Birth, death and horizontal transfer of the fumonisin biosynthetic gene cluster during the evolutionary diversification of *Fusarium*. Mol. Microbiol. 90**,** 290-306.

Rai, R., Cooper, T. G., 2005. In vivo specificity of Ure2 protection from heavy metal ion and oxidative cellular damage in *Saccharomyces cerevisiae*. Yeast 22**,** 343-358.

Rai, R., Tate, J. J., Cooper, T. G., 2003. Ure2, a prion precursor with homology to glutathione S-transferase, protects *Saccharomyces cerevisiae* cells from heavy metal ion and oxidant toxicity. J. Biol. Chem. 278**,** 12826-12833.

Richards, T. A., Leonard, G., Soanes, D. M., Talbot, N. J., 2011. Gene transfer into the fungi. Fungal Biol. Rev. 25**,** 98-110.

Robinson, M. D., McCarthy, D. J., Smyth, G. K., 2010. edgeR: a Bioconductor package for differential expression analysis of digital gene expression data. Bioinformatics 26, 139-140.

Ruepp, A., Zollner, A., Maier, D., Albermann, K., Hani, J., Mokrejs, M., Tetko, I., Guldener, U., Mannhaupt, G., Munsterkotter, M., Mewes, H. W., 2004. The FunCat, a functional annotation scheme for systematic classification of proteins from whole genomes. Nucleic Acids Res. 32, 5539-5545.

Schonknecht, G., Chen, W. H., Ternes, C. M., Barbier, G. G., Shrestha, R. P., Stanke, M., Brautigam, A., Baker, B. J., Banfield, J. F., Garavito, R. M., Carr, K., Wilkerson, C., Rensing, S. A., Gagneul, D., Dickenson, N. E., Oesterhelt, C., Lercher, M. J., Weber, A. P., 2013. Gene transfer from bacteria and archaea facilitated evolution of an extremophilic eukaryote. Science 339, 1207-1210.

Sikhakolli, U. R., Lopez-Giraldez, F., Li, N., Common, R., Townsend, J. P., Trail, F., 2012. Transcriptome analyses during fruiting body formation in *Fusarium graminearum* and *Fusarium verticillioides* reflect species life history and ecology. Fungal Genet. Biol. 49, 663-673.

Slot, J. C., Rokas, A., 2010. Multiple GAL pathway gene clusters evolved independently and by different mechanisms in fungi. Proc. Natl. Acad. Sci. U.S.A. 107, 10136-10141.

Slot, J. C., Rokas, A., 2011. Horizontal transfer of a large and highly toxic secondary metabolic gene cluster between fungi. Curr. Biol. 21, 134-139.

Stajich, J. E., Harris, T., Brunk, B. P., Brestelli, J., Fischer, S., Harb, O. S., Kissinger, J. C., Li, W., Nayak, V., Pinney, D. F., Stoeckert, C. J., Jr., Roos, D. S., 2012. FungiDB: an integrated functional genomics database for fungi. Nucleic Acids Res. 40, D675-681.

Stamatakis, A., 2014. RAxML version 8: a tool for phylogenetic analysis and post-analysis of large phylogenies. Bioinformatics 30**,** 1312-1313.

Stegemann, S., Bock, R., 2009. Exchange of genetic material between cells in plant tissue grafts. Science 324**,** 649-651.

Torruella, G., Suga, H., Riutort, M., Pereto, J., Ruiz-Trillo, I., 2009. The evolutionary history of lysine biosynthesis pathways within eukaryotes. J. Mol. Evol. 69**,** 240-248.

Tsavkelova, E., Oeser, B., Oren-Young, L., Israeli, M., Sasson, Y., Tudzynski, B., Sharon, A., 2012. Identification and functional characterization of indole-3-acetamide-mediated IAA biosynthesis in plant-associated *Fusarium* species. Fungal Genet. Biol. 49**,** 48-57.

Walsh, A. M., Kortschak, R. D., Gardner, M. G., Bertozzi, T., Adelson, D. L., 2013. Widespread horizontal transfer of retrotransposons. Proc. Natl. Acad. Sci. U.S.A. 110**,** 1012-1016.

Walton, J. D., 2000. Horizontal gene transfer and the evolution of secondary metabolite gene clusters in fungi: an hypothesis. Fungal Genet. Biol. 30**,** 167-171.

Wijayawardena, B. K., Minchella, D. J., DeWoody, J. A., 2013. Hosts, parasites, and horizontal gene transfer. Trends Parasitol. 29**,** 329-338.

Wisecaver, J. H., Alexander, W. G., King, S. B., Hittinger, C. T., Rokas, A., 2016. Dynamic evolution of nitric oxide detoxifying flavohemoglobins, a family of single-protein metabolic modules in bacteria and eukaryotes. Mol. Biol. Evol. 33**,** 1979-1987.

Wisecaver, J. H., Rokas, A., 2015. Fungal metabolic gene clusters − caravans traveling across genomes and environments. Front. Microbiol. 6**,** 161.

Wisecaver, J. H., Slot, J. C., Rokas, A., 2014. The evolution of fungal metabolic pathways. PLoS Genet. 10**,** e1004816.

Zabriskie, T. M., Jackson, M. D., 2000. Lysine biosynthesis and metabolism in fungi. Nat. Prod. Rep. 17**,** 85-97.

Zinniel, D. K., Lambrecht, P., Harris, N. B., Feng, Z., Kuczmarski, D., Higley, P., Ishimaru, C. A., Arunakumari, A., Barletta, R. G., Vidaver, A. K., 2002. Isolation and characterization of endophytic colonizing bacteria from agronomic crops and prairie plants. Appl. Environ. Microbiol. 68**,** 2198-2208.

Table 1: Inter-kingdom HGT candidate genes of *F. verticillioides* identified using a phylogenomic pipeline and their respective predicted protein function, distribution within fungi, putative donor group, and potential role in metabolism.

FVEG_ID#[a]	Ch#	Putative function based on NCBI Conserved Domain Database	Fungal distribution[b]	Putative donor[b]	BLASTp identity (%) to highest scoring donor accession	MIPS functional prediction, Metabolism sub-categories[c]
FVEG_00154	1	Dihydrodipicolinate synthase	Pezizomycotina	actinobacteria	64	Lys
FVEG_01713	6	Bifunctional phosphoglucose/phosphomannose isomerase	Pezizomycotina	actinobacteria	72	Unclassified
FVEG_01755*	6	X-Pro dipeptidyl-peptidase	Pezizomycotina	proteobacteria	51	Unclassified
FVEG_03408	5	Sarcosine oxidase	Sordariomycetes	actinobacteria	58	Gly; Lys
FVEG_03450*	2	Glycerophosphodiester phosphodiesterase	*Fusarium* spp.	proteobacteria	77	Unclassified
FVEG_03482	2	Histidinol dehydrogenase	Dikarya	actinobacteria	65	Amino acid
FVEG_03632	2	Arylsulfotransferase	Fungi	actinobacteria	55	Unclassified
FVEG_03648	2	Peptidase family	Sordariomycetes	proteobacteria	64	Unclassified
FVEG_03658	2	Domain of unknown function (DUF1961)	Pezizomycotina	actinobacteria	61	Unclassified
FVEG_03905*	2	Pectate lyase	Dikarya	bacteria	57	Unclassified
FVEG_04320*	4	Carboxylesterase type B	*Fusarium* spp.	proteobacteria	67	Carbohydrate; Sec. metab.
FVEG_05781	3	Phosphoglyceromutase	*Fusarium* spp.	actinobacteria	61	Carbohydrate
FVEG_06712	7	FAD dependent oxidoreductase	Pezizomycotina	proteobacteria	46	Unclassified
FVEG_07753*	8	Cellulase	*Fusarium* spp.	actinobacteria	66	Unclassified
FVEG_08362*	10	Monoamine oxidase	Dikarya	actinobacteria	50	Sec. metab.
FVEG_08761*	10	Glycine/D-amino acid oxidase	Pezizomycotina	proteobacteria	68	Gly; Nitrogen
FVEG_08810	10	D-Glucarate dehydratase	Pezizomycotina	actinobacteria	67	Carbohydrate
FVEG_09347	5	D-Isomer specific 2-hydroxyacid dehydrogenases	Sordariomycetes	bacteria	65	Carbohydrate; Sec. metab.
FVEG_09873	1	Diaminopimelate epimerase	*F. verticillioides*	proteobacteria	69	Lys
FVEG_10127*	9	Arylsulfatase A	Ascomycota	proteobacteria	70	Carbohydrate; Sphingolipid
FVEG_10144	9	Sugar phosphate isomerase/epimerase	Ascomycota	proteobacteria	55	Carbohydrate
FVEG_10494*	11	Type II homoserine kinase; 4-aminobutyrate aminotransferase	*Fusarium* spp.	actinobacteria	76	Gly; Nitrogen
FVEG_10515	11	Acetyl esterase/lipase	Dikarya	actinobacteria	40	Unclassified
FVEG_10637*	11	Dehydrogenase	Sordariomycetes	proteobacteria	56	Carbohydrate; Sec. metab.; Vitamins

FVEG_11008*	9	Monoamine oxidase	Pezizomycotina	actinobacteria	44	Sec. metab.
FVEG_11816	4	Aspartase (L-aspartate ammonia-lyase)	Pezizomycotina	proteobacteria	66	Nitrogen
FVEG_11902*	4	No conserved domain	Pezizomycotina	bacteria	44	Unclassified
FVEG_12189*	4	Alpha-L-fucosidase	Pezizomycotina	actinobacteria	55	Carbohydrate
FVEG_12262	4	Uncharacterized subgroup of the nitrilase superfamily	Fungi	bacteria	70	Nitrogen
FVEG_12273*	4	Alpha/beta hydrolase family	Pezizomycotina	actinobacteria	55	Unclassified
FVEG_12331	4	Glycosyl hydrolase families 32 and 68	Sordariomycetes	actinobacteria	65	Unclassified
FVEG_12843*	11	FAD dependent oxidoreductase	Pezizomycotina	proteobacteria	70	Unclassified
FVEG_13226	6	Acyl esterase	Pezizomycotina	proteobacteria	50	Amino acid
FVEG_13277	6	Sarcosine oxidase	Pezizomycotina	actinobacteria	56	Carbohydrate; Gly; Lys; Nitrogen
FVEG_13461*	8	Phosphoenolpyruvate synthase	Pezizomycotina	proteobacteria	72	Carbohydrate
FVEG_13830	10	Myosin-cross-reactive antigen	Pezizomycotina	actinobacteria	74	Unclassified

[a] The 36 genes determined to be the most robust representatives for inter-kingdom HGT in *F. verticillioides*. The asterisks (*) indicate the 16 genes meeting all criteria, thus being the strongest candidates. The remaining 20 genes met most of the criteria and were considered to be probable HGT candidates.

[b] Distribution of homologs in fungi was determined by NCBI BLASTp. The putative donor group of the homologs to fungi was inferred from BLASTp results and maximum likelihood analysis of gene trees.

[c] The MIPS Functional Catalogue (http://mips.helmholtz-muenchen.de/funcatDB/) was used to identify cellular functions the encoded proteins might confer in *F. verticillioides*, in particular the types of metabolic activity.

Table 2: Distribution of HGT candidates among enriched categories inferred by MIPS Functional Catalogue prediction.

	MIPS Functional Category					
	Metabolism	Glycolysis and gluconeogenesis	Complex cofactor/ co-substrate/ vitamin binding	Electron transport	Activity of intercellular mediators	Peroxisome
Metabolism	21 (2.2[a])					
Glycolysis and gluconeogenesis	2	2 (5.9)				
Complex cofactor/ co-substrate/ vitamin binding	5	0	5 (3.3)			
Electron transport	5	0	3	5 (4.3)		
Activity of intercellular mediators	1	0	0	0	1 (30)	
Peroxisome	2	0	0	2	0	2 (23.5)

[a] Fold enrichment compared to the frequency of such genes within the whole *F. verticillioides* genome.

Table 3: MIPS Functional Catalogue prediction and distribution of HGT candidates in the metabolism sub-categories of amino acid, nitrogen, carbohydrate, sphingolipid, vitamins and cofactors, and secondary metabolites.

	Metabolism Subcategories of MIPS Functional Catalogue					
	Amino acid	Nitrogen	Carbohydrate	Sphingolipid	Vitamins and cofactors	Secondary metabolites
Amino acid	11 (5.9[a])					
Nitrogen	4	6 (6.2)				
Carbohydrate	2	2	10 (2.2)			
Sphingolipid	0	1	1	1 (38.6)		
Vitamins and cofactors	0	0	1	0	1 (24.5)	
Secondary metabolites	2	0	3	0	1	5 (2.6)

[a] Fold enrichment compared to the frequency of such genes within the whole *F. verticillioides* genome.

Table 4: Summary of RNA-Seq analyses of *Fusarium verticillioides* wild type and the FVEG_10494 gene deletion mutant (Δ10494) under nitric oxide stress[a].

	Four different comparisons and the number of differentially expressed genes (up or down)			
	WT treated vs WT non-treated[b]	Mutant treated vs Mutant non-treated[c]	Mutant non-treated vs WT non-treated[d]	Mutant treated vs WT treated[e]
Up-regulated	330	293	0	13
Down-regulated	278	246	1[f]	16[f]

[a] Nitric oxide stress imposed on fungal cultures using 1.5 mM DETA NONOate for 30 min.

[b] Comparison between treated wild type (WT) and non-treated wild type control.

[c] Comparison between treated Δ10494 mutant and non-treated mutant control.

[d] Comparison between non-treated Δ10494 mutant and non-treated wild type.

[e] Comparison between treated Δ10494 mutant and treated wild type.

[f] FVEG_10494 was detected as the only down-regulated gene in the comparison between non-treated Δ10494 mutant and non-treated wild type. In the comparison of treated strains, this gene is one of the 16 down-regulated genes.

Table 5: Differentially expressed genes identified by comparing the FVEG_10494 gene deletion mutant (Δ10494) versus wild type when both were challenged with nitric oxide[a].

Expression Response	FVEG ID#	Log2 Fold Change	Putative Function Based on NCBI Conserved Domain Database
Up-regulated	FVEG_08732	1.33	No putative conserved domains
	FVEG_09672	1.35	No putative conserved domains
	FVEG_09673	1.15	No putative conserved domains
	FVEG_10117	1.23	No putative conserved domains
	FVEG_10576	2.54	No putative conserved domains
	FVEG_10834	1.09	Na(+)/urea-polyamine cotransporter DUR3
	FVEG_11078	1.04	SAM-dependent carboxyl methyltransferase
	FVEG_11079	2.11	Cytochrome P450
	FVEG_11080	1.21	Aldehyde dehydrogenase AldA (AAD23400)-like
	FVEG_11085	1.35	Alpha/beta hydrolases
	FVEG_11086	1.30	Polyketide synthase
	FVEG_15200	1.18	YdcF-like SAM-binding protein
	FVEG_16635	1.19	No putative conserved domains
Down-regulated	FVEG_01304	-1.11	Cys/Met metabolism PLP-dependent enzyme
	FVEG_01376	-1.06	Old yellow enzyme (OYE) YqjM-like FMN binding domain
	FVEG_03830	-.1.19	Glutathione S-transferase
	FVEG_04238	-1.65	Multidrug resistance protein
	FVEG_05981	-1.14	Major facilitator superfamily
	FVEG_07389	-1.11	Nitroreductase-like family 4
	FVEG_08792	-1.86	SRR1 superfamily
	FVEG_09142	-1.29	No putative conserved domains
	FVEG_09386	-1.62	Classical short-chain dehydrogenase/reductase (SDR)
	FVEG_11140	-1.83	Choline dehydrogenase or related flavoprotein
	FVEG_11294	-1.34	Major facilitator superfamily
	FVEG_12249	-1.05	DUF3176 superfamily
	FVEG_12329	-1.59	Sulfate permease or related transporter
	FVEG_13989	-1.09	SMP-30/Gluconolactonase/LRE (SGL) superfamily
	FVEG_15302	-1.35	Classical short-chain dehydrogenase/reductase (SDR)
	FVEG_10494	-13.4	Type II homoserine kinase; 4-aminobutyrate aminotransferase

[a] Nitric oxide stress imposed on fungal cultures using 1.5 mM DETA NONOate for 30 min.

Figure legends

Fig. 1: Phylogenomic pipeline identifying 36 robust inter-kingdom HGT candidates in

Fusarium verticillioides.

The pipeline consisted of a BLAST-based Alien Index screen for HGT candidates, followed by

gene tree construction and two layers of manual curation (see methods section for more details).

A total of 16 and 20 genes were identified as strong and probable HGT candidates, respectively.

Fig. 2: Lysine biosynthesis in *Fusarium verticillioides* and HGT candidates mapped to the

DAP pathway.

The *F. verticillioides* pathways of lysine biosynthesis, including the diaminopimelate (DAP)

pathway (upper branch) and the α-aminoadipate (AAA) pathway (lower branch), were assessed

using the KEGG PATHWAY Database (http://www.genome.jp/kegg/pathway.html). EC

numbers for the enzymes responsible for the corresponding reactions are labeled in the pathways

in rectangular boxes. Enzymes associated with vertically inherited *F. verticillioides* genes are

highlighted in green. Enzymes that are not highlighted lack any known association with a *F.*

verticillioides gene. HGT candidates FVEG_00154 and FVEG_09873 putatively associated with

the DAP pathway are shown in yellow highlighted boxes. They encode a dihydrodipicolinate

synthase (EC 4.3.3.7) and a diaminopimelate epimerase (EC 5.1.1.7), respectively. The vertically

inherited dihydrodipicolinate synthase is encoded by FVEG_05936.

Fig. 3: RAxML phylogeny of *Fusarium verticillioides* FVEG_10494 and other *Fusarium*

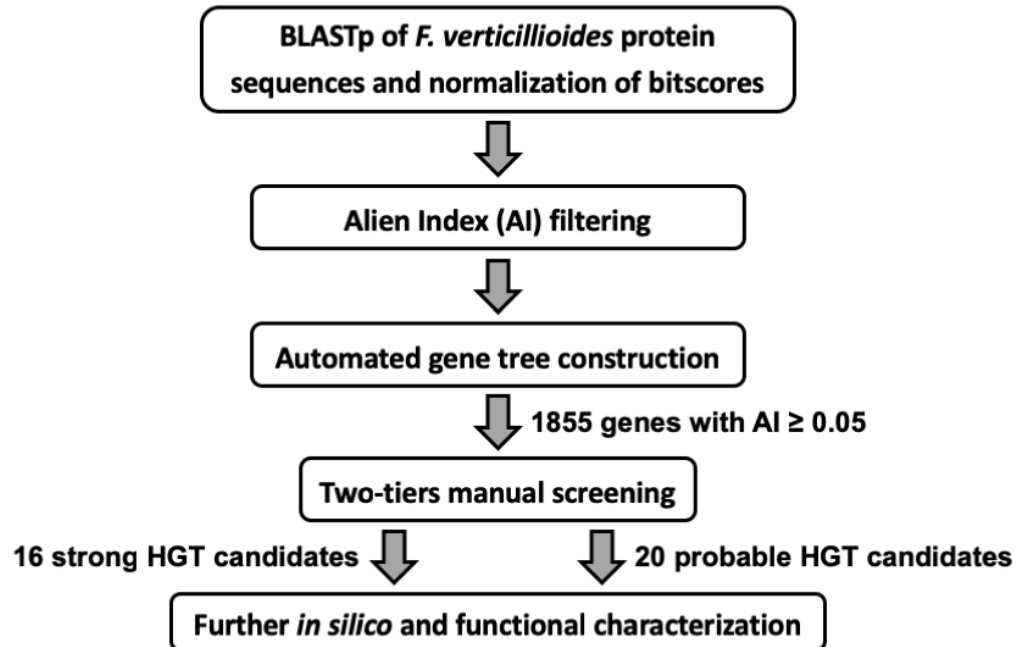**homologs showing close relationship to *Microbacterium testaceum* species.**

Protein sequences of FVEG_10494 and homologs from other *Fusarium* species were aligned to 102 sequences from actinobacteria that were among the best hits from a BLASTp search of the NCBI nr database. The alignment was generated using *MAFFT* and the E-INS-i algorithm, and *RAxML* was used to identify the best scoring maximum likelihood phylogeny (GAMMA LG protein model; 1000 bootstrap replications). Forty accessions from *Mycobacterium* species and 14 accessions from *Streptomyces* species are each shown as collapsed monophyletic clades to conserve space. Only bootstrap values ≥ 80% are shown.

Fig. 4: Abnormal GC content of FVEG_10494 and its high induction under nitric oxide (NO) challenge.

a. GC content was analyzed using Geneious v.8.1.9. The genomic region from FVEG_10490 to FVEG_10498 is shown. Genes are shown as gray rectangles with intervening black lines indicating the intergenic regions. The GC (black line)/AT (gray line) content of the genomic DNA was plotted based on the percentage scale on the left. The GC content of FVEG_10494 is distinctly higher than the surrounding genomic DNA. **b**. Transcriptional analysis of FVEG_10494 under NO stress was performed by challenging a three-day-old PDB culture of wild type with 1.5 mM DETA NONOate for 30 min. Complementary DNA synthesis and qRT-PCR analysis was done in triplicate for each treatment. The $2^{-\Delta\Delta Ct}$ method was used to calculate the relative expression levels. Error bars indicate standard deviations.

Fig. 5: Absence of FVEG_10494 weakens differential expression of genes in response to NO.

Genes down-regulated in the Δ10494 mutant compared to wild type when both were treated with

NO (Table 5) were examined to compare their expression in wild type treated with NO vs.

untreated wild type and in the mutant treated with NO vs. untreated mutant. The level of

differential expression for each gene was less in the mutant comparison compared to the wild

type comparison. Gene ID is labeled on the left and color scale is shown on the right for log2
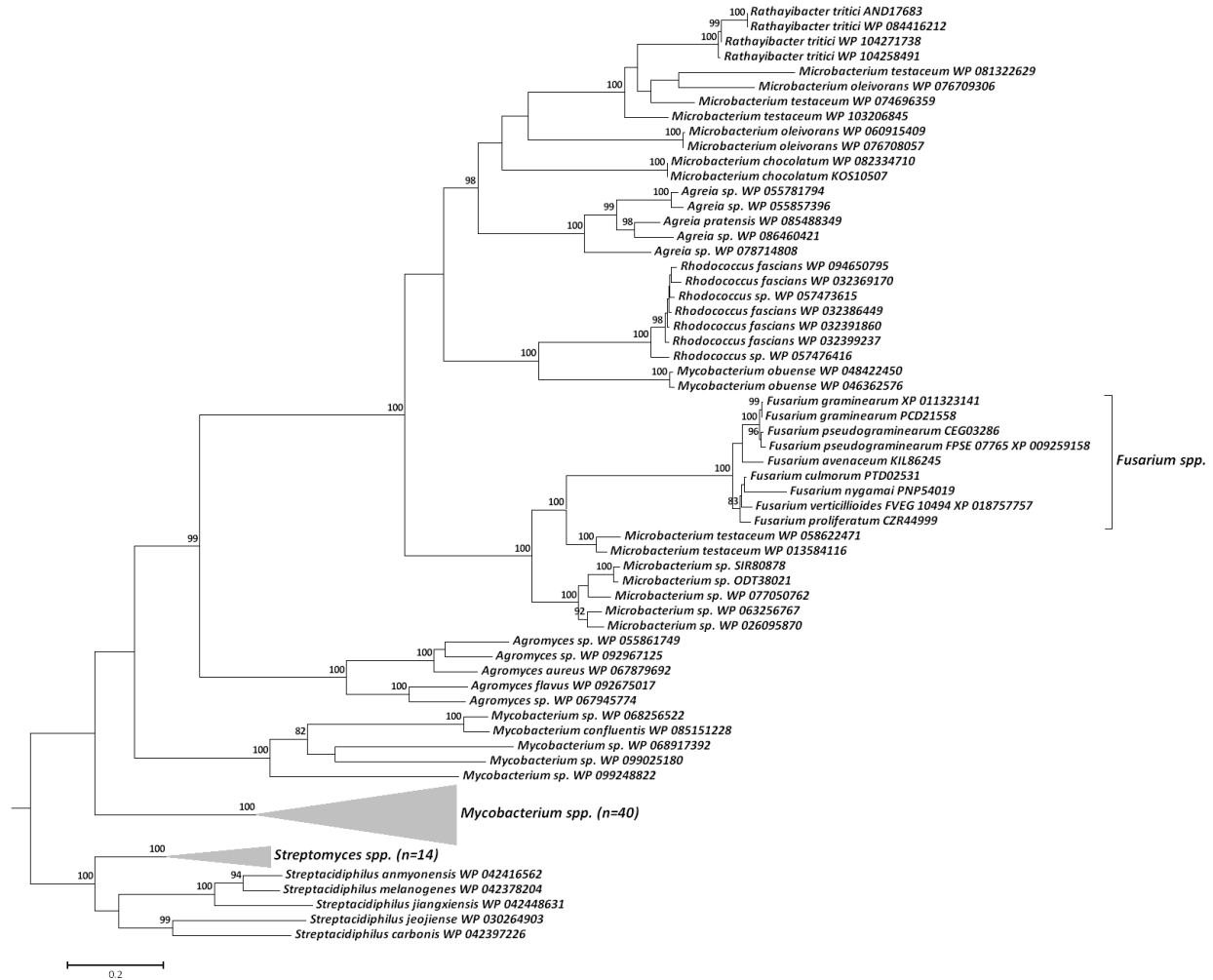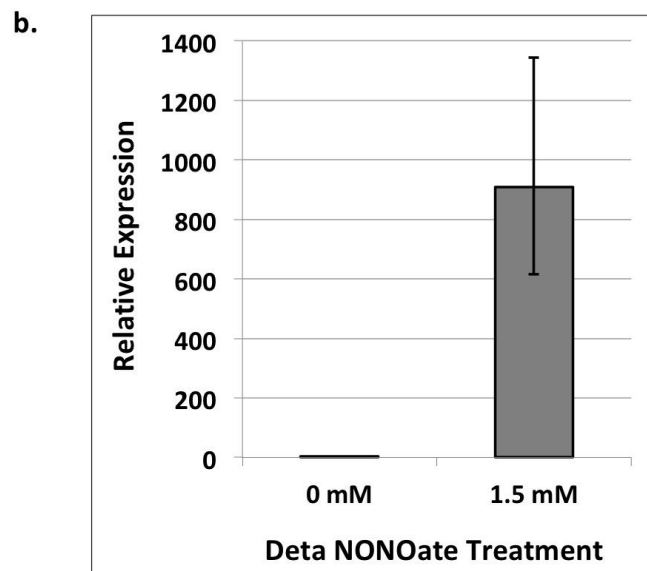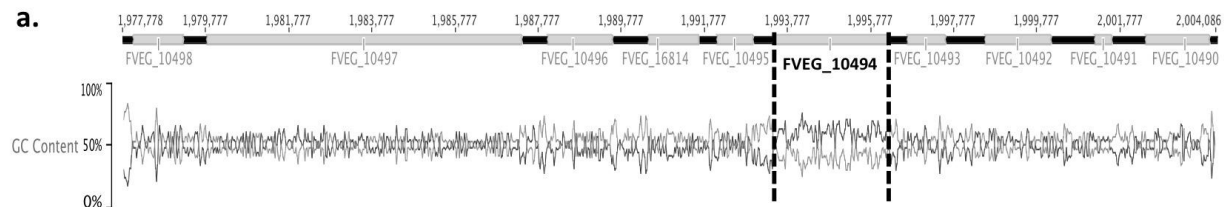
fold change.

a.

b.

Genome-wide analysis of *Fusarium verticillioides* reveals inter-kingdom contribution of horizontal gene transfer to the expansion of metabolism

Shan Gao, Scott E. Gold, Jennifer H. Wisecaver, Yong Zhang, Li Guo, Li-Jun Ma, Antonis Rokas, Anthony E. Glenn

Highlights

- Horizontal gene transfer is implicated in the origin of 36 *F. verticillioides* genes.
- All 36 are putatively derived from bacteria.
- HGT has likely influenced lysine, glycine and nitrogen metabolism.
- One of the genes, FVEG_10494, was highly up-regulated in response to nitric oxide.
- FVEG_10494 moderately enhanced NO-triggered protective responses.
- HGT may allow fungi to expand metabolic capabilities and enhance adaptive strategies.